

Histogram of Gradient Orientations of Signal Plots applied to P300 Detection

Rodrigo Ramele^{1,*}, Ana Julia Villar¹ and Juan Miguel Santos¹

¹*Centro de Inteligencia Computacional, Computer Engineering Department, Instituto Tecnológico de Buenos Aires, Buenos Aires, Argentina*

Correspondence*:

Rodrigo Ramele, C1437FBH Lavarden 315, Ciudad Autónoma de Buenos Aires, Argentina
rramele@itba.edu.ar

2 ABSTRACT

3 Word Count: ~~5132~~-5552

4 The analysis of Electroencephalographic (EEG) signals is of ulterior importance to aid in the
5 diagnosis of mental disease and to increase our understanding of the brain. Traditionally, clinical
6 EEG has been analyzed in terms of temporal waveforms, looking at rhythms in spontaneous
7 activity, subjectively identifying troughs and peaks in Event-Related Potentials (ERP), or by
8 studying graphoelements in pathological sleep stages. Additionally, the discipline of Brain
9 Computer Interfaces requires new methods to decode patterns from non-invasive EEG signals.
10 This field is developing alternative communication pathways to transmit volitional information
11 from the Central Nervous System. The technology could potentially enhance the quality of life
12 of patients affected by neurodegenerative disorders and other mental illness. This work mimics
13 what electroencephalographers have been doing clinically, visually inspecting and categorizing
14 phenomena within the EEG by the extraction of features from images of signal plots. These
15 features are constructed based on the calculation of histograms of oriented gradients from pixels
16 around the signal plot. It aims to provide a new objective framework to analyze, characterize and
17 classify EEG signal waveforms. The feasibility of the method is outlined by detecting the P300, an
18 ERP elicited by the oddball paradigm of rare events, and implementing an offline P300-based BCI
19 Speller. The validity of the proposal is shown by offline processing a public dataset of Amyotrophic
20 Lateral Sclerosis (ALS) patients and an own dataset of healthy subjects.

21 **Keywords:** **electroencephalography, histogram of gradient orientations, brain-computer interfaces, P300, SIFT, amyotrophic lateral**
22 **sclerosis, naive-bayes near neighbours, waveforms**

1 INTRODUCTION

23 Although recent advances in neuroimaging techniques, particularly radio-nuclear and radiological
24 scanning methods (?), have diminished the prospects of the traditional Electroencephalography (EEG),
25 the advent and development of digitized devices has impelled for a revamping of this hundred years old
26 technology. Their versatility, ease of use, temporal resolution, ease of development and production, and
27 its proliferation as consumer devices, are pushing EEG to become the de-facto non invasive portable or
28 ambulatory method to access and harness brain information (?).

29 A key contribution to this expansion has been the field of Brain Computer Interfaces (BCI) (?) which is
30 the pursuit of the development of a new channel of communication particularly aimed to persons affected
31 by neurodegenerative diseases.

32 One noteworthy aspect of this novel communication channel is the ability to transmit information from
33 the Central Nervous System (CNS) to a computer device and from there use that information to control a
34 wheelchair (?), as input to a speller application (?), in a Virtual Reality environment (?) or as aiding tool
35 in a rehabilitation procedure (?). The holly grail of BCI is to implement a new complete and alternative
36 pathway to restore lost locomotion (?).

37 EEG signals are remarkably complex and have been characterized as a multichannel non-stationary
38 stochastic process. Additionally, they have high variability between different subjects and even between
39 different moments for the same subject, requiring adaptive and co-adaptive calibration and learning
40 procedures (?). Hence, this imposes an outstanding challenge that is necessary to overcome in order to
41 extract information from raw EEG signals.

42 BCI has gained mainstream public awareness with worldwide challenge competitions like Cybathlon (??)
43 and even been broadcasted during the inauguration ceremony of the 2014 Soccer World Cup. New
44 developments have overcome the out-of-the-lab high-bar and they are starting to be used in real world
45 environments (??). However, they still lack the necessary robustness, and its performance is well behind
46 any other method of human computer interaction, including any kind of detection of residual muscular
47 movement (?).

48 A few works have explored the idea of exploiting the signal waveform to analyze the EEG signal. In (?)
49 an approach based on Slope Horizontal Chain Code is presented, whereas in (?) a similar procedure
50 was implemented based on Mathematical Morphological Analysis. The seminal work of Bandt-Pompe
51 Permutation Entropy (?) also explores succinctly this idea as a basis to establish the time series ordinal
52 patterns. In the article (?), the authors introduce a method for classification of rhythmic EEG events like
53 Visual Occipital Alpha Waves and Motor Imagery Rolandic Central μ Rhythms using the Histogram
54 of Gradient Orientations of signal plots. Inspired in that work, we propose a novel application of the
55 developed method to classify and describe transient events, particularly the P300 Event Related Potential.
56 The proposed approach is based on the waveform analysis of the shape of the EEG signal. The signal is
57 drawn on a bidimensional image plot, vector gradients of pixels around the plot are obtained, and with
58 them, the histogram of their orientations is calculated. This histogram is a direct representation of the
59 waveform of the signal. The method is built by mimicking what regularly electroencephalographers have
60 been performing for almost a century as it is described in (?): visually inspecting raw signal plots.

61 This paper reports a method to, (1) describe a procedure to capture the shape of a waveform of an ERP
62 component, the P300, using histograms of gradient orientations extracted from images of signal plots,
63 and (2) outline the way in which this procedure can be used to implement an P300-Based BCI Speller
64 application. Its validity is verified by offline processing two datasets, one of data from ALS patients and
65 another one from data of healthy subjects.

66 This article unfolds as follows: Section 2.1 is dedicated to explain the Feature Extraction method based
67 on Histogram of Gradient Orientations of the Signal Plot: Section 2.1.1 shows the preprocessing pipeline,
68 Section 2.1.2 describes the image generation of the signal plot, Section 2.1.3 presents the feature extraction
69 procedure while Section 2.1.4 introduces the Speller Matrix Letter Identification procedure. In Section 2.2,
70 the experimental protocol is expounded. Section 3 shows the results of applying the proposed technique. In
71 the final Section 4 we expose our remarks, conclusions and future work.

2 MATERIALS AND METHODS

The P300 (??) is a positive deflection of the EEG signal which occurs around 300 ms after the onset of a rare and deviant stimulus that the subject is expected to attend. It is produced under the oddball paradigm (?) and it is consistent across different subjects. It has a lower amplitude ($\pm 5\mu V$) compared to basal EEG activity, reaching a Signal to Noise Ratio (SNR) of around -15 db estimated based on the amplitude of the P300 response signal divided by the standard deviation of the background EEG activity (?). This signal can be used to implement a speller application by means of a Speller Matrix (?). This matrix is composed of 6 rows and 6 columns of numbers and letters. The subject can focus on one character of the matrix. Figure 1 shows an example of the Speller Matrix used in the OpenVibe open source software (?), where the flashes of rows and columns provide the deviant stimulus required to elicit this physiological response. Each time a row or a column that contains the desired letter flashes, the corresponding synchronized EEG signal should also contain the P300 signature and by detecting it, the selected letter can be identified.

2.1 Feature Extraction from Signal Plots

In this section, the signal preprocessing, the method for generating images from signal plots, the feature extraction procedure and the Speller Matrix identification are described. Figure 2 shows a scheme of the entire process.

2.1.1 Preprocessing Pipeline

The data obtained by the capturing device is digitalized and a multichannel EEG signal is constructed.

The 6 rows and 6 columns of the Speller Matrix are intensified providing the visual stimulus. The number of a row or column is a location. A sequence of twelve randomly permuted locations l conform an intensification sequence. The whole set of twelve intensifications is repeated k_a times.

• **Signal Enhancement:** This stage consists of the enhancement of the SNR of the P300 pattern above the level of basal EEG. The pipeline starts by applying a notch filter to the raw digital signal, a 4th degree 10 Hz lowpass Butterworth filter and finally a decimation with a Finite Impulse Response (FIR) filter of order 30 from the original sampling frequency down to 16 Hz (?).

• **Artifact Removal:** For every complete sequence of 12 intensifications of 6 rows and 6 columns, a basic artifact elimination procedure is implemented by removing the entire sequence when any signal deviates above/below $\pm 70\mu V$.

• **Segmentation:** For each of the 12 intensifications of one intensification sequence, a segment S_i^l of a window of t_{max} seconds of the multichannel signal is extracted, starting from the stimulus onset, corresponding to each row/column intensification l and to the intensification sequence i . As intensifications are permuted in a random order, the segments are rearranged corresponding to row flickering, labeled 1-6, whereas those corresponding to column flickering are labeled 7-12. Two of these segments should contain the P300 ERP signature time-locked to the flashing stimulus, one for the row, and one for the column.

• **Signal Averaging:** The P300 ERP is deeply buried under basal EEG so the standard approach to identify it is by point-to-point averaging the time-locked stacked signal segments. Hence the values which are not related to, and not time-locked to the onset of the stimulus are canceled out (?).

This last step determines the operation of any P300 Speller. In order to obtain an improved signal in terms of its SNR, repetitions of the sequence of row/column intensification are necessary. And,

at the same time, as long as more repetitions are needed, the ability to transfer information faster is diminished, so there is a trade-off that must be acutely determined.

The procedure to obtain the point-to-point averaged signal goes as follows:

1. Highlight randomly the rows and columns from the matrix. There is one row and one column that should match the letter selected by the subject.
2. Repeat step 1 k_a times, obtaining the $1 \leq l \leq 12$ segments $S_1^l(n, c), \dots, S_{k_a}^l(n, c)$, of the EEG signal where the variables $1 \leq n \leq n_{max}$ and $1 \leq c \leq C$ correspond to sample points and channel, respectively. The parameter C is the number of available EEG channels whereas $n_{max} = F_s t_{max}$ is the segment length and F_s is the sampling frequency. The parameter k_a is the number of repetitions of intensifications and it is an input parameter of the algorithm.
3. Compute the Ensemble Average by

$$x^l(n, c) = \frac{1}{k_a} \sum_{i=1}^{k_a} S_i^l(n, c) \quad (1)$$

for $1 \leq n \leq n_{max}$ and for the channels $1 \leq c \leq C$. This provide an averaged signal $x^l(n, c)$ for the twelve locations $1 \leq l \leq 12$.

2.1.2 Signal Plotting

Averaged signal segments are standardized and scaled for $1 \leq n \leq n_{max}$ and $1 \leq c \leq C$ by

$$\tilde{x}^l(n, c) = \left\lfloor \gamma \frac{(x^l(n, c) - \bar{x}^l(c))}{\hat{\sigma}^l(c)} \right\rfloor \quad (2)$$

where $\gamma > 0$ is an input parameter of the algorithm and it is related to the image scale. In addition, $x^l(n, c)$ is the point-to-point averaged multichannel EEG signal for the sample point n and for channel c . Lastly,

$$\bar{x}^l(c) = \frac{1}{n_{max}} \sum_{n=1}^{n_{max}} x^l(n, c)$$

and

$$\hat{\sigma}^l(c) = \sqrt{\left\{ \frac{1}{n_{max}-1} \sum_{n=1}^{n_{max}} \left[x^l(n, c) - \bar{x}^l(c) \right]^2 \right\}}$$

are the mean and estimated standard deviation of $x^l(n, c)$, $1 \leq n \leq n_{max}$, for each channel c .

Consequently, a binary image $I^{(l,c)}$ is constructed according to

$$I^{(l,c)}(z_1, z_2) = \begin{cases} 255 & \text{if } z_1 = \gamma n \quad \text{and} \quad z_2 = \tilde{x}^l(n, c) + z^l(c) \\ 0 & \text{otherwise} \end{cases} \quad (3)$$

with 255 being white and representing the signal's value location and 0 for black which is the background contrast, conforming a black-and-white plot of the signal. Pixel arguments $(z_1, z_2) \in \mathbb{N} \times \mathbb{N}$ iterate over the width (based on the length of the signal segment) and height (based on the peak-to-peak amplitude) of the newly created image with $1 \leq n \leq n_{max}$ and $1 \leq c \leq C$. The value $z^l(c)$ is the image vertical position

132 where the signal's zero value has to be situated in order to fit the entire signal within the image for each
 133 channel c:

$$z^l(c) = \left\lfloor \frac{\max_n \tilde{x}^l(n, c) - \min_n \tilde{x}^l(n, c)}{2} \right\rfloor - \left\lfloor \frac{\max_n \tilde{x}^l(n, c) + \min_n \tilde{x}^l(n, c)}{2} \right\rfloor \quad (4)$$

134 where the minimization and maximization are carried out for n varying between $1 \leq n \leq n_{max}$, and $\lfloor \cdot \rfloor$
 135 denote the rounding to the smaller nearest integer of the number.

136 In order to complete the plot $I^{(l,c)}$ from the pixels, the Bresenham (??) algorithm is used to interpolate
 137 straight lines between each pair of consecutive pixels.

138 2.1.3 Feature Extraction: Histogram of Gradient Orientations

139 The work of Edelman, Intrator and Poggio (?) on how the visual cortex sense features was the inspiration
 140 to the development of an algorithm to identify and decode salient local information from image regions.
 141 The Scale Invariant Feature Transform (SIFT) is a Computer Vision method proposed by ? which is
 142 composed of two parts, the SIFT Detector and the SIFT Descriptor. The former is the procedure to identify
 143 relevant areas of an image whereas the latter is the procedure to describe and characterize a region of an
 144 image (i.e. patch) calculating an histogram of the gradient orientations. In order to characterize EEG
 145 signal waveforms, this work proposes an alternative to the SIFT Descriptor, the Histogram of Gradient
 146 Orientations algorithm. We stripped away all the details which are not used and refined the procedure to
 147 enable the effective capturing of the waveform shape.

148 For each generated image $I^{(l,c)}$, a keypoint p_k is placed on a pixel (x_{p_k}, y_{p_k}) over the image plot and a
 149 window around the keypoint is considered. A local image patch of size $X_p \times X_p$ pixels is constructed by
 150 dividing the window in 16 blocks of size $3s$ each one, where s is the scale of the local patch and it is an
 151 input parameter of the algorithm. It is arranged in a 4×4 grid and the pixel p_k is the patch center, thus
 152 $X_p = 12s$ pixels.

153 A local representation of the signal shape within the patch can be described by obtaining the gradient
 154 orientations on each of the 16 blocks $B_{i,j}$ with $0 \leq i, j \leq 3$ and creating a histogram of gradients. This
 155 technique is based on Lowe's SIFT (?) method, and it is biomimetically inspired in how the visual cortex
 156 detects shapes by analyzing orientations (?). In order to calculate the histogram, the interval $[0, 360]$ of
 157 possible angles is divided in 8 bins, each one of 45 degrees.

158 Hence, for each spatial bin $0 \leq i, j \leq 3$, corresponding to the indexes of each block $B_{i,j}$, the orientations
 159 are accumulated in a 3-dimensional histogram h through the following equation:

$$h(\theta, i, j) = 3s \sum_{\mathbf{p} \in I^{(l,c)}} w_{ang}(\angle J(\mathbf{p}) - \theta) w_{ij} \left(\frac{\mathbf{p} - \mathbf{p}_k}{3s} \right) \left\| J(\mathbf{p}) \right\| \quad (5)$$

160 where \mathbf{p} is a pixel from the image $I^{(l,c)}$, θ is the angle bin with $\theta \in \{0, 45, 90, 135, 180, 225, 270, 315\}$,
 161 $|J(\mathbf{p})|$ is the norm of the gradient vector in the pixel \mathbf{p} and it is computed using finite differences
 162 and $\angle J(\mathbf{p})$ is the angle of the gradient vector. The

163 The contribution of each gradient vector to the histogram calculated by Equation 5 is balanced by a
 164 trilinear interpolation. The scalar $w_{ang}(\cdot)$ and vector $w_{ij}(\cdot)$ functions are linear interpolations used by ?

165 and ? to provide a weighting contribution to the eight adjacent bins in the tridimensional histogram. They
 166 are calculated as

$$w_{ij}(\mathbf{v}) = w(v_x - x_i)w(v_y - y_j) \quad (6)$$

167 with $0 \leq i, j \leq 3$ and

$$w_{\text{ang}}(\alpha) = \sum_{r=-1}^1 w\left(\frac{8\alpha}{2\pi} + 8r\right) \quad (7)$$

168 where x_i and y_i are the spatial bin centers located in $x_i, y_j \in \{-\frac{3}{2}, -\frac{1}{2}, \frac{1}{2}, \frac{3}{2}\}$, and the interpolating
 169 function $w(\cdot)$ is defined as $w(z) = \max(0, |z| - 1)$. The function parameter $\mathbf{v} = (v_x, v_y)$ is a vector
 170 variable and α a scalar variable. Vector \mathbf{v} holds pixel coordinates (v_x, v_y) normalized between -2 and
 171 2 and combined with the function $w(z)$ it produces zero for every combination of (i, j) except for the 4
 172 adjacent spatial bins. On the other hand, r is an integer that can vary freely between $[-1, 1]$ which allows the
 173 argument in the set $\{-1, 0, 1\}$ and α to be unconstrained in terms of its values in radians. The interpolating
 174 function $w(\cdot)$ is defined as $w(z) = \max(0, |z| - 1)$ is the difference between the gradient orientation angle
 175 and the angle bin center in radians. By following this procedure, summands on Equation 7 are nullified
 176 except for the 2 adjacent angular bins.

177 These binning functions conform a the trilinear interpolation that has a combined effect of sharing the
 178 contribution of each oriented gradient between their eight adjacent bins in a tridimensional cube in the
 179 histogram space, and zero everywhere else (?).

180 Lastly, the fixed value of 3 is a magnification factor which corresponds to the number of pixels per each
 181 block when $s = 1$. As the patch has 16 blocks and 8 bin angles are considered, for each location l and
 182 channel c a feature called descriptor $\mathbf{d}^{(l,c)}$ of 128 dimension is obtained.

183 Figure 3 shows an example of a patch and a scheme of the histogram computation. In (A) a plot of the
 184 signal and the patch centered around the keypoint is shown. In (B) the possible orientations on each patch
 185 are illustrated. Only the upper-left four blocks are visible. The first eight orientations of the first block, are
 186 labeled from 1 to 8 clockwise. The orientations of the second block $B_{1,2}$ are labeled from 9 to 16. This
 187 labeling continues left-to-right, up-down until the eight orientations for all the sixteen blocks are assigned.
 188 They form the corresponding descriptor \mathbf{d} of 128 coordinates. Finally, in (C) an enlarged image plot is
 189 shown where the oriented gradient vector for each pixel can be seen.

190 2.1.4 Speller Matrix letter Identification

191 2.1.4.1 P300 ERP Extraction

192 Segments corresponding to row flickering are labeled 1-6, whereas those corresponding to column
 193 flickering are labeled 7-12. The extraction process has the following steps:

- 194 • **Step A:** First highlight rows and columns from the matrix in a random permutation order and obtain
 195 the Ensemble Average as detailed in steps 1, 2 and 3 in Section 2.1.1.
- 196 • **Step B:** Plot the signals $\tilde{x}^l(n, c)$, $1 \leq n \leq n_{\max}$, $1 \leq c \leq C$, according Section 2.1.2 in order to
 197 generate the images $I^{(l,c)}$ for rows and columns $1 \leq l \leq 12$.

- 198 • Step C: Obtain the descriptors $\mathbf{d}^{(l,c)}$ for rows and columns from $I^{(l,c)}$ in accordance to the method
 199 described in Section 2.1.3.

200 **2.1.4.2 Calibration**

201 A trial, as defined by the BCI2000 platform (?), is every attempt to select just one letter from the speller.
 202 A set of trials is used for calibration and once the calibration is complete it can be used to identify new
 203 letters from new trials.

204 During the calibration phase, two descriptors $\mathbf{d}^{(l,c)}$ are extracted for each available channel, corresponding
 205 to the locations l of a selection of one previously instructed letter from the set of calibration trials. These
 206 descriptors are the P300 templates, grouped together in a template set called T^c . The set is constructed
 207 using the steps described in Section 2.1.1 and the steps A, B and C of the P300 ERP extraction process.

208 Additionally, the best performing channel, bpc is identified based on the the channel where the best
 209 Character Recognition Rate is obtained.

210 **2.1.4.3 Letter identification**

211 In order to identify the selected letter, the template set T^{bpc} is used as a database. Thus, new ~~descriptors~~
 212 ~~unclassified descriptors~~ $\mathbf{q}^{(l,bpc)}$ are computed and they are compared against the descriptors belonging to
 213 the calibration template set T^{bpc} .

214 ~~The Naive Bayes Nearest Neighbor (k-NBNN) (?) is a discriminative (?) semi-supervised classification~~
 215 ~~algorithm that allows the categorization of an image to one class by comparing the set of extracted~~
 216 ~~descriptors to those which are more similar from template dictionaries. This work proposes an adapted~~
 217 ~~version to obtain a unary classification scheme to identify the selected letter in the P300-Based BCI~~
 218 ~~Speller, based on the features provided by the calculated descriptors.~~

- 219 • Step D: Match to the calibration template T^{bpc} by computing

$$\hat{row} = \arg \min_{l \in \{1, \dots, 6\}} \sum_{q \in N_T(\mathbf{d}^{(l,bpc)})} \sum_{h=1}^k \left\| \mathbf{q}^{(l,bpc)} - \mathbf{d}_{h}^{(l,bpc)} \right\|^2 \quad (8)$$

220 and

$$\hat{col} = \arg \min_{l \in \{7, \dots, 12\}} \sum_{q \in N_T(\mathbf{d}^{(l,bpc)})} \sum_{h=1}^k \left\| \mathbf{q}^{(l,bpc)} - \mathbf{d}_{h}^{(l,bpc)} \right\|^2 \quad (9)$$

221 ~~where $N_T(\mathbf{d}^{(l,bpc)})$ is defined as $N_T(\mathbf{d}^{(l,bpc)}) = \{\mathbf{d} \in T^{bpc} / \mathbf{d}$ is the k-nearest neighbor of $\mathbf{d}^{(l,bpc)}$ } with~~
 222 ~~$\mathbf{d}_h^{(bpc)}$ belonging to the set $N_T(\mathbf{q}^{(l,bpc)})$, which is defined, for the best performing channel, as~~
 223 ~~$N_T(\mathbf{q}^{(l,bpc)}) = \{\mathbf{d}_h^{(bpc)} \in T^{bpc} / \mathbf{d}_h^{(bpc)}$ is the k-nearest neighbor of $\mathbf{q}^{(l,bpc)}$ }~~. This set is obtained by
 224 sorting all the elements in T^{bpc} based on distances between them and $\mathbf{d}^{(l,bpc)} \mathbf{q}^{(l,bpc)}$, choosing the k
 225 with smaller values, with k a parameter of the algorithm. ~~This procedure is based on the k-NBNN~~
 226 ~~algorithm (?)~~.

227 By computing the aforementioned equations, the letter of the matrix can be determined from the intersection
 228 of the row \hat{row} and column \hat{col} . Figure 2 shows a scheme of this process.

229 2.2 Experimental Protocol

230 To verify the validity of the proposed framework and method, the public dataset 008-2014 (?) published
231 on the BNCI-Horizon website (?) by IRCCS Fondazione Santa Lucia, is used. Additionally, an own dataset
232 with the same experimental conditions is generated. Both of them are utilized to perform an offline BCI
233 Simulation to decode the spelled words from the provided signals.

234 The algorithm is implemented ~~using VLFeat (?) Computer Vision libraries on MATLAB V2014a on~~
235 ~~MATLAB V2017a~~ (Mathworks Inc., Natick, MA, USA). ~~The algorithm described in 2.1.3 is implemented~~
236 ~~on a modified version of the VLFeat (?) Computer Vision library~~. Furthermore, in order to enhance the
237 impact of ~~our this~~ paper and for a sake of reproducibility, the code of the ~~algorithm entire algorithm~~,
238 ~~including the modified VLFeat library~~, has been made available at: <https://bitbucket.org/itba/hist>.

239 In the following sections the characteristics of the datasets and parameters of the identification algorithm
240 are described.

241 2.2.1 P300 ALS Public Dataset

242 The experimental protocol used to generate this dataset is explained in (?) but can be summarized as
243 follows: 8 subjects with confirmed diagnoses but on different stages of ALS disease, were recruited and
244 accepted to perform the experiments. The Visual P300 detection task designed for this experiment consisted
245 of spelling 7 words of 5 letters each, using the traditional P300 Speller Matrix (?). The flashing of rows
246 and columns provide the deviant stimulus required to elicit this physiological response. The first 3 words
247 are used for calibration and the remaining 4 words, for testing with visual feedback. A trial is every attempt
248 to select a letter from the speller. It is composed of signal segments corresponding to $k_a = 10$ repetitions
249 of flashes of 6 rows and $k_a = 10$ repetitions of flashes of 6 columns of the matrix, yielding 120 repetitions.
250 Flashing of a row or a column is performed for 0.125s, following by a resting period (i.e. inter-stimulus
251 interval) of the same length. After 120 repetitions an inter-trial pause is included before resuming with the
252 following letter.

253 The recorded dataset was sampled at 256 Hz and it consisted of a scalp multichannel EEG signal for
254 electrode channels Fz, Cz, Pz, Oz, P3, P4, PO7 and PO8, identified according to the 10-20 International
255 System, for each one of the 8 subjects. The recording device was a research-oriented digital EEG device
256 (g.Mobilab, g.Tec, Austria) and the data acquisition and stimuli delivery were handled by the BCI2000
257 open source software (?).

258 In order to assess and verify the identification of the P300 response, subjects are instructed to perform a
259 copy-spelling task. They have to fix their attention to successive letters for copying a previously determined
260 set of words, in contrast to a free-running operation of the speller where each user decides on its own what
261 letter to choose.

262 2.2.2 P300 for healthy subjects

263 We replicate the same experiment on healthy subjects using a wireless digital EEG device (g.Nutilus,
264 g.Tec, Austria). The experimental conditions are the same as those used for the previous dataset, as detailed
265 in section 2.2.1. The produced dataset is available in a public online repository (?).

266 Participants are recruited voluntarily and the experiment is conducted anonymously in accordance with
267 the Declaration of Helsinki published by the World Health Organization. No monetary compensation
268 is handed out and all participants agree and sign a written informed consent. This study is approved
269 by the *Departamento de Investigación y Doctorado, Instituto Tecnológico de Buenos Aires (ITBA)*. All

270 healthy subjects have normal or corrected-to-normal vision and no history of neurological disorders. The
 271 experiment is performed with 8 subjects, 6 males, 2 females, 6 right-handed, 2 left-handed, average age
 272 29.00 years, standard deviation 11.56 years, range 20-56 years.

273 EEG data is collected in a single recording session. Participants are seated in a comfortable chair, with
 274 their vision aligned to a computer screen located one meter in front of them. The handling and processing
 275 of the data and stimuli is conducted by the OpenVibe platform (?).

276 Gel-based active electrodes (g.LADYbird, g.Tec, Austria) are used on the same positions Fz, Cz, Pz,
 277 Oz, P3,P4, PO7 and PO8. Reference is set to the right ear lobe and ground is preset as the AFz position.
 278 Sampling frequency is slightly different, and is set to 250 Hz, which is the closest possible to the one used
 279 with the other dataset.

280 2.2.3 Parameters

281 The patch size is $X_P = 12s \times 12s$ pixels, where s is the scale of the local patch and it is an input parameter
 282 of the algorithm. The P300 event can have a span of 400 ms and its amplitude can reach $10\mu V$ (?). Hence
 283 it is necessary to utilize a signal segment of size $t_{max} = 1$ second and a size patch X_P that could capture
 284 an entire transient event. With this purpose in consideration, the s value election is essential.

285 We propose the Equations 10 and 11 to compute the scale value in horizontal and vertical directions,
 286 respectively.

$$s_x = \frac{\gamma \lambda F_s}{12} \quad (10)$$

$$s_y = \frac{\gamma \Delta\mu V}{12} \quad (11)$$

287 where λ is the length in seconds covered by the patch, F_s is the sampling frequency of the EEG signal
 288 (downsampled to 16 Hz) and $\Delta\mu V$ corresponds to the amplitude in microvolts that can be covered by the
 289 height of the patch. The geometric structure of the patch forces a squared configuration, then we discerned
 290 that by using $s = s_x = s_y = 3$ and $\gamma = 4$, the local patch and the descriptor can identify events of $9\mu V$
 291 of amplitude, with a span of $\lambda = 0.56$ seconds. This also determines that 1 pixel represents $\frac{1}{\gamma} = \frac{1}{4}\mu V$ on
 292 the vertical direction and $\frac{1}{F_s \gamma} = \frac{1}{64}$ seconds on the horizontal direction. The keypoints p_k are located at
 293 $(x_{p_k}, y_{p_k}) = (0.55F_s \gamma, z^l(c)) = (35, z^l(c))$ for the corresponding channel c and location l (see Equation 4).
 294 In this way the whole transient event is captured. Figure 4 shows a patch of a signal plot covering the
 295 complete amplitude (vertical direction) and the complete span of the signal event (horizontal direction).

296 **LastyMoreover**, the number of channels C is equal to 8 for both datasets, and the number of
 297 intensification sequences k_a is fixed to 10. The parameter k used to construct the set $N_T(\mathbf{d}^{(l,c)})$ is assigned
 298 to $k = 7$, which was found empirically to achieve better results. In addition, the norm used on Equations 8
 299 and 9 is the cosine norm, and descriptors are normalized to $[-1, 1]$.

300 **Lastly, in order to assess the validity of the Histogram of Gradient Orientations (HIST) method, the**
 301 **character recognition rate for both datasets is evaluated replicating the methodology proposed by the**
 302 **ALS dataset's publisher, since authors ? did not report the Character Recognition Rate obtained for**
 303 **this dataset. Frequency filtering, data segmentation and artifact rejection is conducted according to**
 304 **Section 2.1.1 yielding 16 x 8 samples per epoch. A multichannel feature consists of time points vector (?),**
 305 **formed by concatenating all the channels (?). A single-channel variant consists of using time points**
 306 **from a single electrode and performing the analysis on a channel-by-channel basis. Three classification**

307 schemes are considered as well. A multichannel version of the Stepwise Linear Discriminant Analysis
308 (SWLDA) classification algorithm, SWLDA is the methodology proposed by the ALS dataset's publisher.
309 Additionally, a single-channel and a multichannel variant of a linear kernel Support Vector Machine
310 (SVM) (?) classifier are utilized. SVM has been successfully used in several BCI Competitions (?).

3 RESULTS

311 Table 1 shows the results of applying the **Histogram of Gradient Orientations (HIST)** HIST algorithm to
312 the subjects of the public dataset of ALS patients. The percentage of correctly spelled letters is calculated
313 while performing an offline BCI Simulation. From the seven words for each subject, the first three are used
314 for calibration, and the remaining four are used for testing. The best performing channel *bpc* is informed
315 as well. The target ratio is 1 : 36; hence theoretical chance level is 2.8%. It can be observed that the best
316 performance of the letter identification method is reached in a dissimilar channel depending on the subject
317 being studied. Table 1 and 2 show for comparison the obtained performance rates using single-channel
318 signals with the **Support Vector Machine (SVM)** (?) classifier. This method is configured to use a linear
319 kernel. SVM classifier. The best performing channel, where the best letter identification rate was achieved,
320 is also depicted.

321 The Information Transfer Rate (ITR), or Bit Transfer Rate (BTR), in the case of reactive BCIs (?)
322 depends on the amount of signal averaging required to transmit a valid and robust selection. Figure 5 shows
323 the performance curves for varying intensification sequences for the subjects included in the dataset of
324 ALS patients. It can be noticed that the percentage of correctly identified letters depends on the number
325 of intensification sequences that are used to obtain the averaged signal. Moreover, when the number of
326 intensification sequences tend to 1, which corresponds to single-intensification character recognition, the
327 performance is reduced. As mentioned before, the SNR of the P300 obtained from only one segment of the
328 intensification sequence is very low and the shape of its P300 component is not very well defined.

329 In Table 2 the results obtained for 8 healthy subjects are shown. It can be observed that the performance is
330 above chance level. It was is verified that HIST method has an improved performance at letter identification
331 than SVM that process the signals on a channel by channel strategy (Wilcoxon signed-rank test, $p = 0.004$
332 for both datasets).

333 Tables 3 and 4 are presented in order to compare the performance of the HIST method versus a
334 multichannel version of the Stepwise Linear Discriminant Analysis (SWLDA) multichannel SWLDA
335 and SVM classification algorithms for both datasets. The feature was formed by concatenating all the
336 channels (?). SWLDA is the methodology proposed by the ALS dataset's publisher. Since authors ? did
337 not report the Character Recognition Rate obtained for this dataset, we replicate their procedure and
338 include the performance obtained with the SWLDA algorithm at letter identification. It was It is verified
339 for the dataset of ALS patients that it has similar performance against other methods like SWLDA or SVM,
340 which use a multichannel feature (Quade test with $p = 0.55$) whereas for the dataset of healthy subjects
341 significant differences were are found (Quade test with $p = 0.02$) where only the HIST method achieved
342 achieves a different performance than SVM (with multiple comparisons, significant difference of level
343 0.05).

344 The P300 ERP consists of two overlapping components: the P3a and P3b, the former with frontocentral
345 distribution while the later stronger on centroparietal region (?). Hence, the standard practice is to find
346 the stronger response on the central channel Cz (?). However, ? show that the response may also arise in

347 occipital regions. We found that by analyzing only the waveforms, occipital channels PO8 and PO7 show
348 higher performances for some subjects.

349 As subjects have varying *latencies* and *amplitudes* of their P300 components, they also have a varying
350 stability of the *shape* of the generated ERP (?). Figure 6 shows 10 sample P300 templates patches for
351 patients 8 and 3 from the dataset of ALS patients. It can be discerned that in coincidence with the
352 performance results, the P300 signature is more clear and consistent for subject 8 (A) while for subject 3
353 (B) the characteristic pattern is more difficult to perceive.

354 Additionally, the stability of the P300 component waveform has been extensively studied in patients
355 with ALS (?????) where it was found that these patients have a stable P300 component, which were also
356 sustained across different sessions. In line with these results we do not find evidence of a difference in
357 terms of the performance obtained by analyzing the waveforms (HIST) for the group of patients with ALS
358 and the healthy group of volunteers (Mann-Whitney U Test, $p = 0.46$). Particularly, the best performance
359 is obtained for a subject from the ALS dataset for which, based on visual observation, the shape of their
360 P300 component is consistently identified.

361 It is important to remark that when applied to binary images obtained from signal plots, the feature
362 extraction method described in Section 2.1.3 generates sparse descriptors. Under this subspace we found
363 that using the cosine metric yielded a significant performance improvement. On the other hand, the unary
364 classification scheme based on the NBNN algorithm proved very beneficial for the P300 Speller Matrix.
365 This is due to the fact that this approach solves the unbalance dataset problem which is inherent to the
366 oddball paradigm (?).

4 DISCUSSION

367 Among other applications of Brain Computer Interfaces, the goal of the discipline is to provide
368 communication assistance to people affected by neuro-degenerative diseases, who are the most likely
369 population to benefit from BCI systems and EEG processing and analysis.

370 In this work, a method to extract an objective metric from the waveform of the plots of EEG signals is
371 presented. Its usage to implement a valid P300-Based BCI Speller application is expounded. Additionally,
372 its validity is evaluated using a public dataset of ALS patients and an own dataset of healthy subjects.

373 It was verified that this method has an improved performance at letter identification than other methods
374 that process the signals on a channel by channel strategy, and it even has a comparable performance against
375 other methods like SWLDA or SVM, which uses a multichannel feature. Furthermore, this method has the
376 advantage that shapes of waveforms can be analyzed in an objective way. We observed that the shape of
377 the P300 component is more stable in occipital channels, where the performance for identifying letters
378 is higher. We additionally verified that ALS P300 signatures are stable in comparison to those of healthy
379 subjects.

380 We believe that the use of descriptors based on histogram of gradient orientation, presented in this work,
381 can also be utilized for deriving a shape metric in the space of the P300 signals which can complement
382 other metrics based on time-domain as those defined by ?. It is important to notice that the analysis of
383 waveform shapes is usually performed in a qualitative approach based on visual inspection (?), and a
384 complementary methodology which offer a quantitative metric will be beneficial to these routinely analysis
385 of the waveform of ERPs.

386 The goal of this work is to answer the question if a P300 component could be solely determined by
387 inspecting automatically their waveforms. We conclude affirmatively, though two very important issues
388 still remain:

389 First, the stability of the P300 in terms of its shape is crucial: the averaging procedure, montages, the
390 signal to noise ratio and spatial filters all of them are non-physiological factors that affect the stability of
391 the shape of the P300 ERP. We tested a preliminary approach to assess if the morphological shape of the
392 P300 of the averaged signal can be stabilized by applying different alignments of the stacked segments (see
393 Figure 2) and we verified that there is a better performance when a correct segment alignment is applied.
394 We applied Dynamic Time Warping (DTW) (?) to automate the alignment procedure but we were unable
395 to find a substantial improvement. Further work to study the stability of the shape of the P300 signature
396 component needs to be addressed.

397 The second problem is the amplitude variation of the P300. We propose a solution by standardizing the
398 signal, shown in Equation 2. It has the effect of normalizing the peak-to-peak amplitude, moderating its
399 variation. It has also the advantage of reducing noise that was not reduced by the averaging procedure. It is
400 important to remark that the averaged signal variance depends on the number of segments used to compute
401 it (?). The standardizing process converts the signal to unit signal variance which makes it independent of
402 the number k_a of signals averaged. Although this is initially an advantageous approach, the standardizing
403 process reduces the amplitude of any significant P300 complex diminishing its automatic interpretation
404 capability.

405 To further extend the capabilities of this method, it would be desirable to implement a multichannel
406 version. The straightforward extension of concatenating the obtained descriptors results in high
407 dimensional feature vector, while other variants that merge descriptors per channel may diminish the
408 mutual information between different channels. Hitherto variants using color versions of SIFT (?), where
409 different color bands are mapped to electrode channels, have been explored without substantial success.

410 In our opinion, the best benefit of the presented method is that a closer collaboration of the field of
411 BCI with physicians can be fostered (?), since this procedure intent to imitate human visual observation.
412 Automatic classification of patterns in EEG that are specifically identified by their shapes like K-Complex,
413 Vertex Waves, Positive Occipital Sharp Transient (?) are a prospect future work to be considered. We are
414 currently working in unpublished material analyzing K-Complex components that could eventually provide
415 assistance to physicians to locate these EEG patterns, specially in long recording periods, frequent in sleep
416 research (?). Additionally, it can be used for artifact removal which is performed on many occasions by
417 visually inspecting signals. This is due to the fact that the descriptors are a direct representation of the shape
418 of signal waveforms. In line with these applications, it can be used to build a database (?) of quantitative
419 representations of waveforms and improve atlases (?), which are currently based on qualitative descriptions
420 of signal shapes.

CONFLICT OF INTEREST STATEMENT

421 The authors declare that the research was conducted in the absence of any commercial or financial
422 relationships that could be construed as a potential conflict of interest.

AUTHOR CONTRIBUTIONS

423 This work is part of the PhD thesis of RR which is directed by JS and codirected by AV.

FUNDING

424 This project was supported by the ITBACyT-15 funding program issued by ITBA University from Buenos
 425 Aires, Argentina.

Table 1. Character recognition rates for the public dataset of ALS patients using the Histogram of Gradient (HIST) calculated from single-channel plots. Performance rates using single-channel signals with the SVM classifier are shown for comparison. The best performing channel *bpc* for each method is visualized

Participant		bpc	HIST	bpc	Single Channel SVM
1	Cz	35%	Cz		15%
2	Fz	85%	PO8		25%
3	Cz	25%	Fz		5%
4	PO8	55%	Oz		5%
5	PO7	40%	P3		25%
6	PO7	60%	PO8		20%
7	PO8	80%	Fz		30%
8	PO7	95%	PO7		85%

Table 2. Character recognition rates for the own dataset of healthy subjects using the Histogram of Gradient (HIST) calculated from single-channel plots. Performance rates using single-channel signals with the SVM classifier are shown for comparison. The best performing channel *bpc* for each method is visualized.

Participant		bpc	HIST	bpc	Single Channel SVM
1	Oz	40%	Cz		10%
2	PO7	30%	Cz		5%
3	P4	40%	P3		10%
4	P4	45%	P4		35%
5	P4	60%	P3		10%
6	Pz	50%	P4		25%
7	PO7	70%	P3		30%
8	P4	50%	PO7		10%

Table 3. Character recognition rates and the best performing channel bpc for the public dataset of ALS patients using the Histogram of Gradient (HIST) (repeated here for comparison purposes). Performance rates obtained by SWLDA and SVM classification algorithms with a multichannel concatenated feature.

Participant	bpc for HIST	HIST	Multichannel SWLDA	Multichannel SVM
1	Cz	35%	45%	40%
2	Fz	85%	30%	50%
3	Cz	25%	65%	55%
4	PO8	55%	40%	50%
5	PO7	40%	35%	45%
6	PO7	60%	35%	70%
7	PO8	80%	60%	35%
8	PO7	95%	90%	95%

Table 4. Character recognition rates and the best performing channel bpc for the own dataset of healthy subjects using the Histogram of Gradient (HIST) (repeated here for comparison purposes). Performance rates obtained by SWLDA and SVM classification algorithms with a multichannel concatenated feature.

Participant	bpc for HIST	HIST	Multichannel SWLDA	Multichannel SVM
1	Oz	40%	65%	40%
2	PO7	30%	15%	10%
3	P4	40%	50%	25%
4	P4	45%	40%	20%
5	P4	60%	30%	20%
6	Pz	50%	35%	30%
7	PO7	70%	25%	30%
8	P4	50%	35%	20%

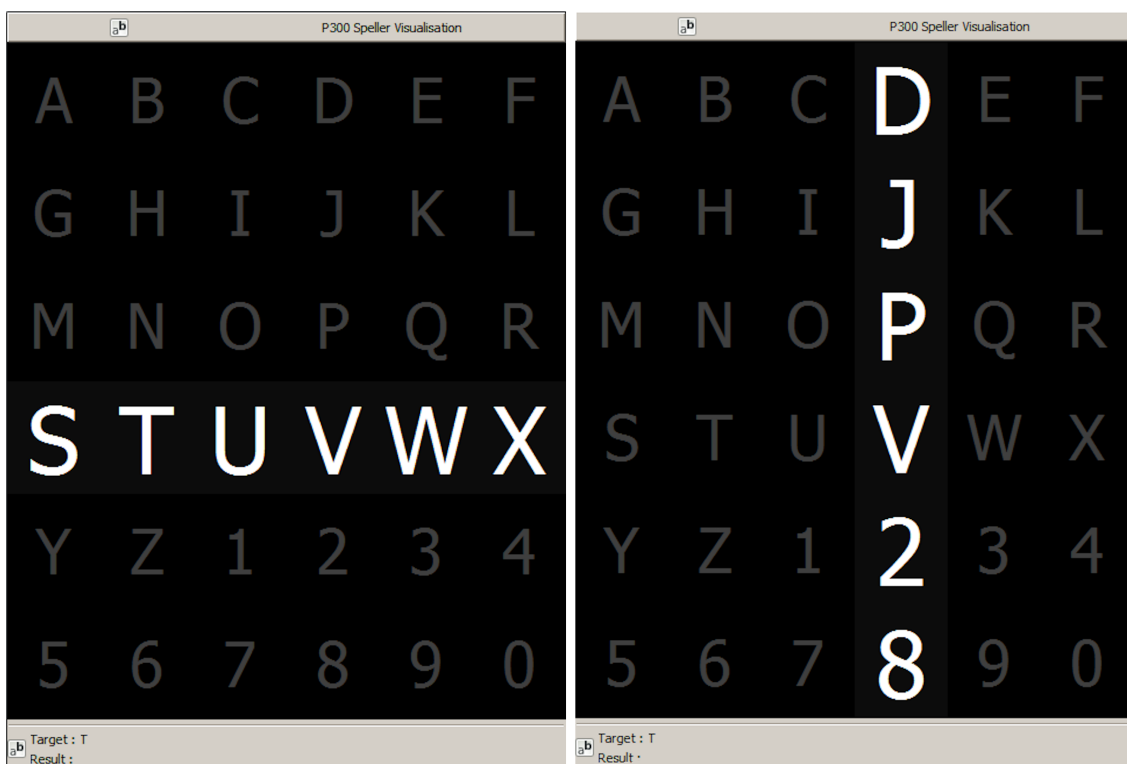


Figure 1. Example of the 6×6 Speller Matrix used in the study obtained from the OpenVibe software. Rows and columns flash in random permutations.

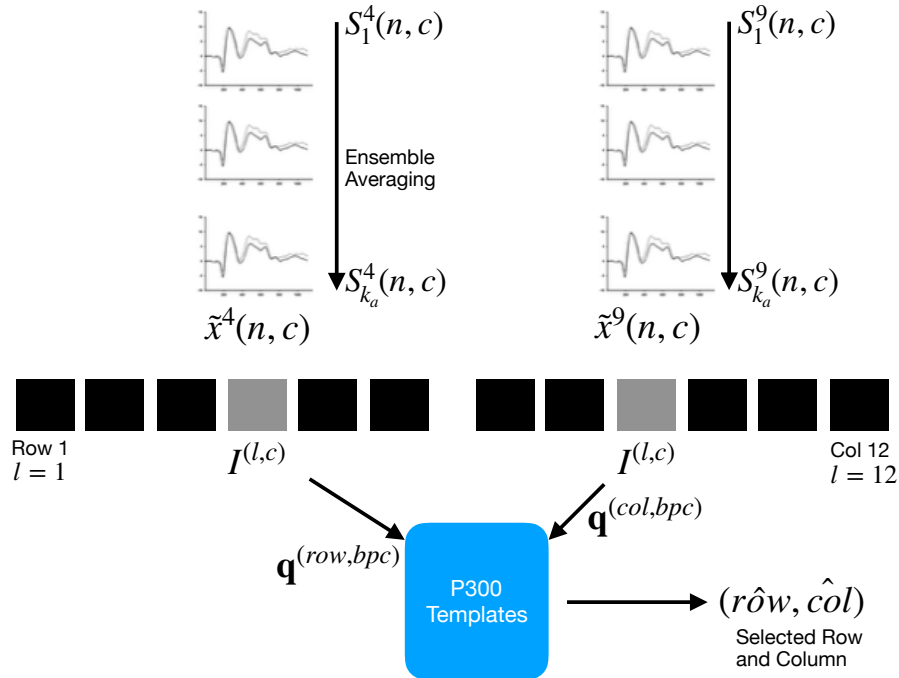


Figure 2. For each column and row, an averaged, standardized and scaled signal $\tilde{x}^l(n, c)$ is obtained from the segments S_i^l corresponding to the k_a intensification sequences with $1 \leq i \leq k_a$ and location l varying between 1 and 12. From the averaged signal, the image $I^{(l,c)}$ of the signal plot is generated and each descriptor is computed. By comparing each descriptor against the set of templates, the P300 ERP can be detected, and finally the desired letter from the matrix can be inferred.

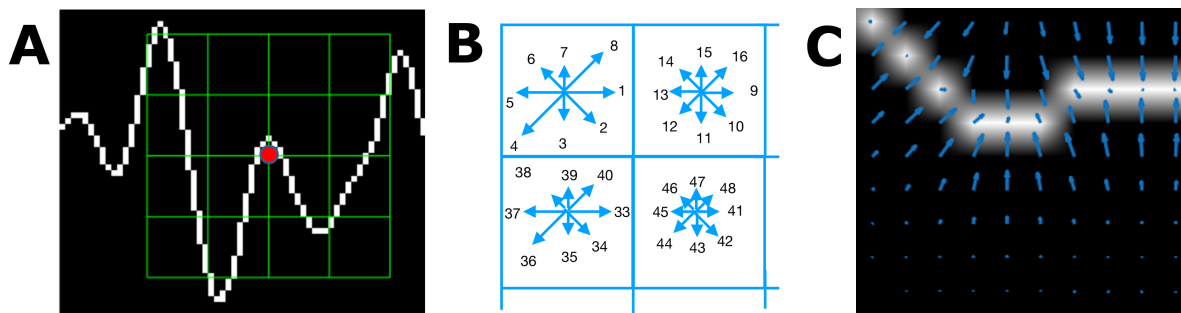


Figure 3. (A) Example of a plot of the signal, a keypoint and the corresponding patch. (B) A scheme of the orientation's histogram computation. Only the upper-left four blocks are visible. The first eight orientations of the first block, are labeled from 1 to 8 clockwise. The orientation of the second block $B_{1,2}$ is labeled from 9 to 16. This labeling continues left-to-right, up-down until the eight orientations for all the sixteen blocks are assigned. They form the corresponding descriptor of 128 coordinates. The length of each arrow represent the value of the histogram on each direction for each block. (C) Vector field of oriented gradients. Each pixel is assigned an orientation and magnitude calculated using finite differences.

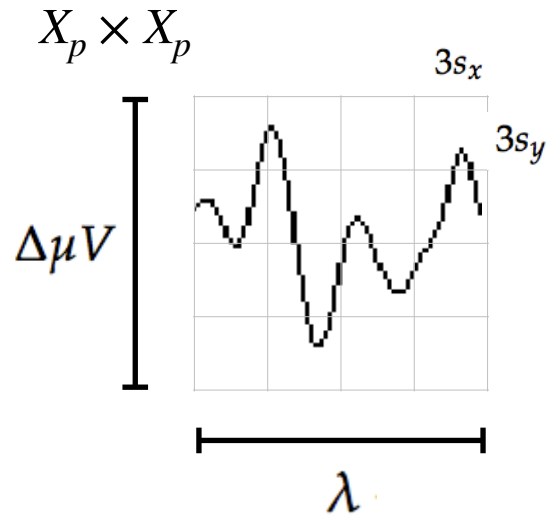


Figure 4. The scale of local patch is selected in order to capture the whole transient event. The size of the patch is $X_p \times X_p$ pixels. The vertical size consists of 4 blocks of size $3s_y$ pixels which is high enough as to contain the signal $\Delta\mu V$, the peak-to-peak amplitude of the transient event. The horizontal size includes 4 blocks of $3s_x$ and covers the entire duration in seconds of the transient signal event, λ .

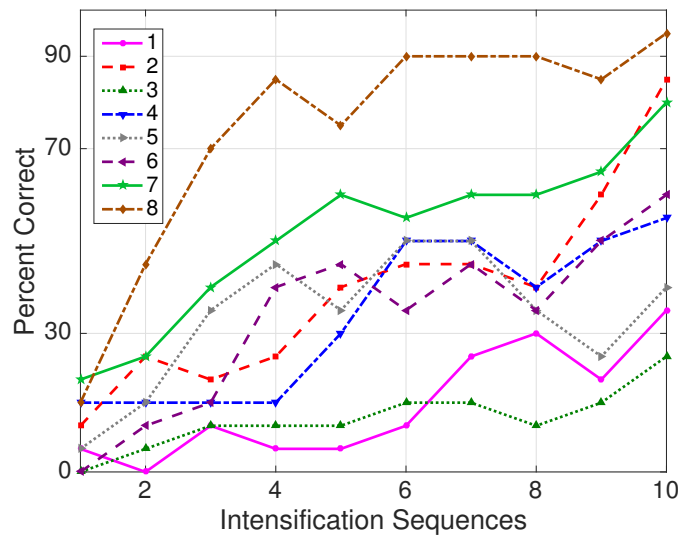


Figure 5. Performance curves for the eight subjects included in the dataset of ALS patients. Three out of eight subjects achieved the necessary performance to implement a valid P300 speller.

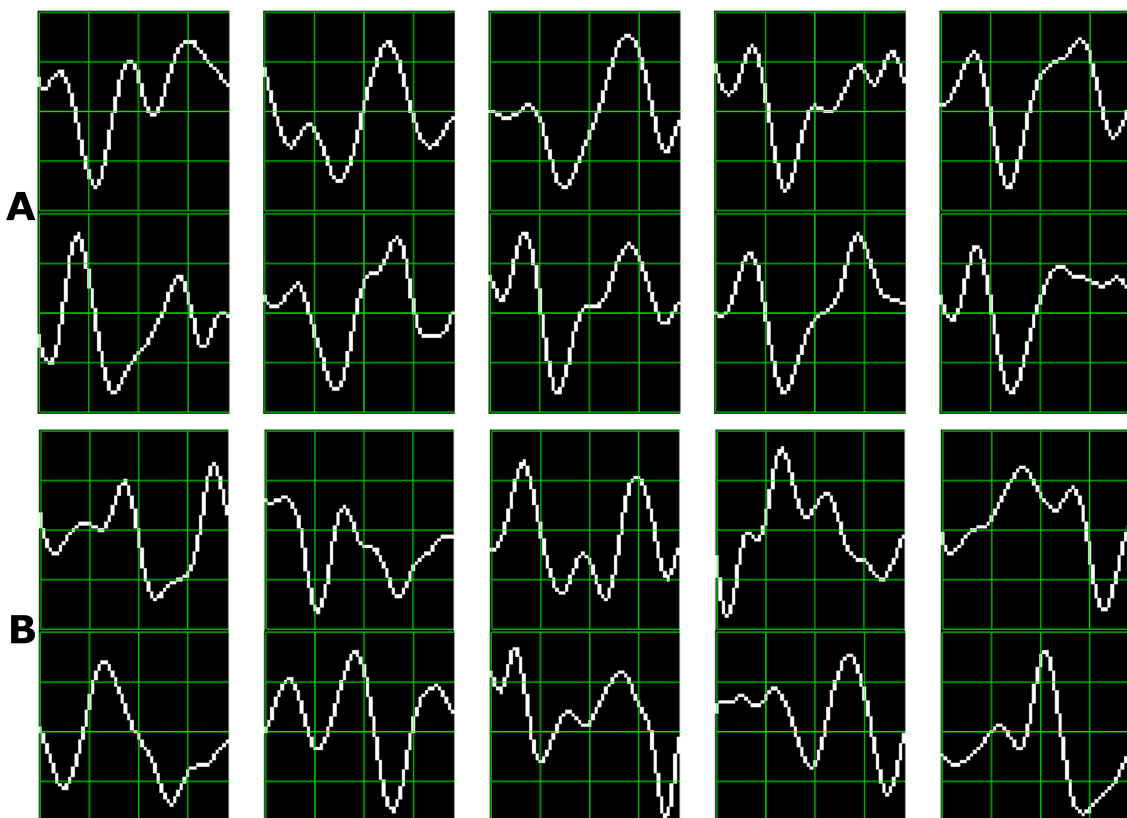


Figure 6. Ten sample P300 template patches for subjects 8 (A) and 3 (B) of the ALS Dataset. Downward deflection is positive polarity.